Received: 12 June 2019 | Revised: 10 September 2019 | Accepted: 9 October 2019

DOI: 10.1002/stem.3113

TISSUE-SPECIFIC STEM CELLS

STEM CELLS

Extracellular vesicles transmit epithelial growth factor activity in the intestinal stem cell niche

Ádám Oszvald[1] | Zsuzsanna Szvicsek[1] | Gyöngyvér Orsolya Sándor[1] | Andrea Kelemen[1] | András Áron Soós[1] | Krisztina Pálóczi[1] | Attila Bursics[2] | Kristóf Dede[2] | Tamás Tölgyes[2] | Edit I. Buzás[1,3,4] | Anikó Zeöld[1] | Zoltán Wiener[1]

[1]Department of Genetics, Cell and Immunobiology, Semmelweis University, Budapest, Hungary

[2]Uzsoki Hospital Budapest, Budapest, Hungary

[3]MTA-SE Immune-Proteogenomics Extracellular Vesicle Research Group, Semmelweis University, Budapest, Hungary

[4]HCEMM-SE Extracellular Vesicle Research Group, Budapest, Hungary

Correspondence
Zoltán Wiener, PhD, Department of Genetics, Cell and Immunobiology, Semmelweis University, H-1085, Budapest, Üllői út 26, Hungary.
Email: wiener.zoltan@med.semmelweis-univ.hu

Funding information
Ministry of Human Capacities, Hungary, Grant/Award Numbers: VEKOP-2.3.3-15-2017-00016, VEKOP-2.3.2-16-2017-000002, National Excellence Program in Higher Education (SE); National Research, Development and Innovation Office, Hungary, Grant/Award Numbers: NVKP_16-0007, OTKA 120237, OTKA 111958, OTKA-NN 118018; International Centre for Genetic Engineering and Biotechnology, Italy, Grant/Award Number: CRP/HUN16-04_EC

Abstract

Extracellular vesicles (EV) are membrane-surrounded vesicles that represent a novel way of intercellular communication by carrying biologically important molecules in a concentrated and protected form. The intestinal epithelium is continuously renewed by a small proliferating intestinal stem cell (ISC) population, residing at the bottom of the intestinal crypts in a specific microenvironment, the stem cell niche. By using 3D mouse and human intestinal organoids, we show that intestinal fibroblast-derived EVs are involved in forming the ISC niche by transmitting Wnt and epidermal growth factor (EGF) activity. With a mouse model that expresses EGFP in the Lgr5+ ISCs, we prove that loss in ISC number in the absence of EGF is prevented by fibroblast-derived EVs. Furthermore, we demonstrate that intestinal fibroblast-derived EVs carry EGF family members, such as amphiregulin. Mechanistically, blocking EV-bound amphiregulin inhibited the EV-induced survival of organoids. In contrast, EVs have no role in transporting R-Spondin, a critical niche factor amplifying Wnt signaling. Collectively, we prove the important role of fibroblast-derived EVs as a novel transmission mechanism of factors in the normal ISC niche.

KEYWORDS

amphiregulin, exosomes, extracellular vesicle, fibroblast, intestinal stem cell, Lgr5, organoid, Wnt

1 | INTRODUCTION

The intestinal epithelium is continuously renewed by a proliferating stem cell population, residing at the bottom of the intestinal crypts in a specific microenvironment, the stem cell niche. The intestinal stem cell (ISC) population can be characterized by the expression of the Lgr5 protein[1] that acts by mediating Wnt signal enhancement via soluble R-Spondin proteins.[2] ISCs critically depend on niche factors, derived from the microenvironment, such as from intestinal fibroblasts or Paneth cells in the small intestine. Lgr5^{+} mouse small intestinal crypt stem cells self-organize into continuously renewing organoids in 3D matrix ex vivo when stimulated by the niche factors epidermal growth factor (EGF), the bone morphogenic protein (Bmp) pathway inhibitor noggin and the Wnt-agonist R-Spondin1.[3,4] In addition, colonic organoids require the addition of Wnt proteins, such as Wnt3a as well.[3] Unlike the traditional cell lines, these 3D cultures

maintain the spatial cellular composition similar to the in vivo situation and they produce all the differentiated cell types, thus, providing an excellent and well-controlled experimental system to dissect factors important in shaping the intestinal epithelium.

Extracellular vesicles (EVs) are membrane-enclosed structures, secreted by both normal and cancer cells. The largest EVs are the apoptotic bodies released by cells undergoing apoptosis. Microvesicles are directly shed from the plasma membrane, whereas exosomes (EXs), the best characterized and smallest EV subpopulation, are derived from the multivesicular bodies (MVB) of the endosomal compartment and they are released from cells upon fusion of the MVBs with the plasma membrane.[5] Since the pure isolation of different EV subpopulations according to their intracellular origin is not yet resolved, EVs are often categorized based on their size as small and large EVs.[6] EVs transfer a wide array of biologically important molecules, such as proteins, lipids, mRNAs, and miRNAs in a concentrated form when they target the recipient cells,[5,7] and the roles of mesenchymal stem cell-derived and mesenchymal stromal cell-derived EVs, for example, have already been intensively studied.[8,9]

Despite the increasing knowledge how ISC niche is formed, not many studies have so far been published on the way of transmitting ISC niche factors. In a recent report, the short-range Wnt gradient among ISCs and Paneth cells has been visualized.[10] Importantly, EVs provide locally a high concentration of the delivered molecules; thus, they may be a very efficient transmission tool in the ISC niche. In line with this notion, previous studies showed that macrophage-derived EVs enhance stem cell survival after radiation injury via delivering Wnt proteins.[11] Furthermore, a recent study reported that EVs are critically involved in the regeneration of the intestinal epithelium after injuries by transporting Annexin A1.[12] However, the role of EVs in shaping the ISC niche under homeostatic condition is still poorly understood. In the present study, we have found that intestinal fibroblasts, a critical cell type in shaping the ISC niche, release EVs with Wnt and EGF activity; furthermore, EGF family members, such as amphiregulin, are active on the surface of EVs. All together, these results show that EVs represent a novel mechanism of transmitting ISC niche signals and fibroblast-derived EVs critically contribute to maintaining the ISC phenotype.

Significance Statement

Intestinal stem cells (ISC) reside in a specific microenvironment in the intestinal epithelium, the ISC niche. Although they are critical in maintaining tissue integrity, the transmission of ISC niche factors is still not well known. Extracellular vesicles (EV) carry biologically active molecules in a membrane-surrounded form, thus, representing a novel way of intercellular communication. The present article provides evidence that fibroblast-derived EVs transport epidermal growth factor activity, one of the critical niche factors, by carrying amphiregulin; thus, they represent a novel way of intercellular signal transmission mechanism for normal ISCs.

2 | MATERIALS AND METHODS

2.1 | Cell culture

Human colon fibroblasts (American Tissue Culture Collection, ATCC-1459) (HCFs) were cultured in DMEM with 4500 g/L glucose (DMEM high glucose, Gibco-Thermo Fisher Scientific, Waltham, MA), 10% fetal bovine serum (FBS; Biosera, France), glutamine and Penicillin/Streptomycin (Gibco). When collecting EVs, cells were washed with phosphate-buffered saline (PBS) three times and cultured in serum-free medium or in incomplete SI medium for 2 days. Incomplete SI medium contained advanced Dulbecco's modified Eagle's medium (DMEM)/F12 with N2 and B27 supplement (Gibco), 10 mM N-2-hydroxyethylpiperazine-N′-2-ethanesulfonic acid (HEPES; Sigma, St Louis, MO), 1 μM N-Acetyl-Cysteine (Sigma), glutamine, penicillin/streptomycin, and antibiotic/antimycotic mix (Gibco). Cells were then removed from tissue culture plates (Eppendorf, Austria) with TrypLE (Gibco) and counted in a Burker chamber. Cell cultures were tested for mycoplasma contamination with Hoechst staining, and they were negative in our experiments. We used only cells with low passage number (<p9 after obtaining from ATCC).

2.2 | Isolation of murine small intestinal fibroblasts

Small intestines were opened, washed with PBS, and cut into small pieces (<0.5 cm) in PBS. After extensive washing steps, tissue pieces were incubated in 2 mM ethylenediaminetetraacetic acid (EDTA) for 30 minutes at 4°C. Crypts with epithelial cells were then mechanically removed, and tissue pieces were washed to replace EDTA. They were suspended in DMEM high glucose, 10% FBS, antibiotic/antimycotic mix and glutamine containing 75 U/mL collagenase II (Sigma), 125 μg/mL collagenase and dispase mix (Roche, Switzerland) and incubated for 60–120 minutes at 37°C. Supernatant with single cells was centrifuged at 300*g* for 5 minutes, washed twice with PBS, and cells were then cultured in fibroblast medium (DMEM high glucose supplemented with 15% FBS, ciprofloxacin [Sigma, 1:200 dilution], antibiotic/antimycotic mix and glutamine).

2.3 | Mouse intestinal crypt cultures

The veterinary authority (Pest County Government Office, Hungary) approved the experiments with mice. Intestinal crypts from C57Bl/6J (Jackson Laboratory) or *Lgr5-EGFP-IRES-Cre^{ER}* mice (Jackson Laboratory, 008875) were isolated according to previously published methods.[4,13] Approximately 1000 crypts were embedded into growth factor-reduced, phenol red-free Matrigel (Corning, NY, 20 μL/well or 40 μL/well in 48 or 24-well plates, respectively) and cultured in incomplete SI medium supplemented with 100 ng/mL noggin (Peprotech, Rocky Hill, NJ), 50 ng/mL EGF (Peprotech), and 500 ng/mL mouse R-Spondin1 (R&D Systems-Bio-Techne, Minneapolis, MN) (complete SI medium). In case of colonic crypts, 100 ng/mL murine Wnt3a (Peprotech) was included as well (colonic medium). Organoids were removed from Matrigel in every

4–6 days, mechanically disrupted by pipetting, centrifuged at 300*g* for 5 minutes, and they were then embedded into new Matrigel. In some experiments, the GSK-3 inhibitor CHIR99021 (Sigma) was dissolved in DMSO (Sigma) and applied at 3 μM for >3 days.

To produce *Apc*-mutant organoids, we used a previously published sgRNA sequence (sgRNA4),[14] and cloned it into the lentiCRISPR v2 plasmid (Addgene 52961). Apc-mutant organoids were produced according to Schwank et al and Szvicsek et al,[14,15] and they were selected by removing R-Spondin1, EGF, and noggin 3 days after transfection. *Apc*-mutant organoids were used >6 days culturing them without growth factors.

2.4 | Human colon organoid cultures

The Medical Research Council of Hungary (ETT-TUKEB) approved all experiments with human samples, and informed consent was obtained from the patients (men aged 63, 76, and 68 years). Normal colon tissue samples were collected from patients undergoing colorectal cancer surgical operation, where a distance of more than 3 cm to the tumors was used.[3] Human colonic crypts were isolated according to Sato et al[3] with some modifications. Briefly, samples were cut into <0.5 cm pieces, washed with PBS five times, and incubated in PBS + 2 mM EDTA (Sigma) for 30 minutes at 4°C in tubes that had been coated with 0.1% bovine serum albumin (BSA, Sigma). Fractions were then taken with PBS + 0.1% BSA into tubes containing 3 mL advanced DMEM/F12 medium (Gibco). Fractions with crypts were embedded into Matrigel droplets (20 μL/well, 48-well plate, Eppendorf) and cultured in human organoid medium containing advanced DMEM/F12 with N2 and B27 supplements, 10 mM HEPES, 1 mM N-Acetyl-Cysteine, glutamine, antibiotic/antimycotic mix, 500 nM A83-01 (Sigma), 10 μM SB202190-Monohydrochloride (Sigma), 50 ng/mL human EGF, 100 ng/mL human noggin (Peprotech), 1000 ng/mL human R-Spondin1 (R&D Systems), 100 ng/mL murine Wnt3a (Peprotech), and 1 nM gastrin (Sigma). For treatment with EVs, organoids were isolated from Matrigel by centrifugation at 300*g* for 5 minutes, mechanically disrupted and embedded into 3D matrix again.

2.5 | Flow cytometry

Cells were removed with TrypLE (Gibco) and they were fixed with 4% paraformaldehyde (PFA) for 20 minutes. They were permeabilized with 0.1% saponin (BD Biosciences, Franklin Lakes, NJ) and labeled with αSma antibody for 30 minutes and then with Alexa 488-labeled secondary antibody for 20 minutes. After washing in PBS and centrifugation at 300*g* for 5 minutes, 10 000 events were measured on a FACSCalibur flow cytometer (BD Biosciences). The list of antibodies can be found in the Supporting Information Appendix.

2.6 | EV isolation and functional tests with EVs

Cell culture supernatants were collected after 2 days and serially centrifuged at 300*g* for 5 minutes, 2000*g* for 20 minutes, and 12 500*g* for 20 minutes to remove cells, cell debris, and the larger EVs. EVs were isolated with ultracentrifugation (UC) at 100 000*g* for 70 minutes at 4°C, the pellet was washed with PBS, ultracentrifuged again and then resuspended in culture media. EVs from approximately 3×10^5 fibroblasts were added to each well with organoids (20 μL Matrigel, 200 μL total medium). This contained 4.8×10^8 (±16.3% SD, n = 3) particles according to Nanoparticle Tracking Analysis measurements (see below). In some experiments, EVs were incubated with 10 μg/mL control goat IgG or anti-amphiregulin antibody (see Supporting Information Appendix) for 1 hour in 20 μL medium before applying them to organoids.

2.7 | Tunable resistive pulse sensing (qNano) measurements

Supernatants from fibroblasts cultured in serum-free fibroblast medium were collected after 48 hours, centrifuged at 300*g* for 5 minutes, at 2000*g* for 20 minutes, and at 12 500*g* for 20 minutes. EVs were collected by UC, the pellet was resuspended in DMEM medium and then further diluted in PBS. Samples were applied to tunable resistance pulse sensing analysis (qNano, Izon, UK), minimum 500 data points were collected, or samples were measured for 5 minutes. CPC200B (Izon) beads were used for particle size and concentration calibration, and they were diluted in the same ratio of medium and PBS when applying membranes with a pore size of 200 nm (analysis range: 85–500 nm).

2.8 | Nanoparticle tracking analysis

Samples after UC were resuspended in 1 mL PBS, and particle size distribution and concentration were recorded on a ZetaView Z-NTA instrument (Particle Metrix, Germany). For each measurement, 11 cell positions were scanned at 25°C with the following camera settings: auto expose, gain: 28.8, offset: 0, shutter: 100, sensitivity: 80. The videos were analyzed by the ZetaView Analyze software 8.05.10 with a minimum area of 5, maximum area of 1000, and a minimum brightness of 20.

2.9 | Protein concentration measurement and Simple Western (WES) analysis

HCFs were cultured in serum-free medium for 2 days, and the cell number was counted by a Burker chamber. EVs were pelleted with UC at 100 000 g for 70 minutes at 4°C, they were washed with PBS, ultracentrifuged again, and then dissolved in 19 μL CelLytic M buffer (Sigma) and 1 μL cOmplete Protease Inhibitor Cocktail (Roche). The lysates were subjected to two freeze-thaw cycles, they were sonicated for 10 minutes, centrifuged at 14,000*g* for 15 minutes, and protein concentrations of the supernatants were measured with the Micro BCA Protein Assay Kit (Thermo Fisher Scientific, Waltham, MA) and NanoDrop ND-1000 spectrophotometer (Thermo Fisher Scientific). Of note, 3 μL of the lysates containing 1.5 μg protein were applied to capillary-based Simple Western analysis WES

(ProteinSimple, San Jose, CA) according to the manufacturer's instructions. As a control, we used 3 μL of the lysate prepared from ultracentrifuged serum-free medium. The following kits were used (ProteinSimple): SM-W004 (for analysis between 12 and 230 kDa), DM-TP01 total protein detection kit, DM-001 anti-rabbit detection kit, DM-006 anti-goat detection kit, and PS-ST02EZ-8 EZ Standard Pack 2. The primary antibodies are listed in the Supporting Information Appendix. The results were analyzed by the Compass for SW 4.0.1 software (ProteinSimple).

2.10 | Human EV detection by anti-CD63 or anti-CD81-coated beads

Fibroblast culture supernatants were harvested after 2 days. They were centrifuged at 300*g* for 5 minutes, 2000*g* for 20 minutes, and 12 500*g* for 20 minutes. EVs were then bound to antibody-coated beads that had been blocked with 0.1% BSA (Sigma) for 30 minutes. Of note, 20 and 6 μL of anti-CD63 coated beads (Thermo Fisher Scientific, 10606D) or anti-CD81 coated beads (Thermo Fisher Scientific, 10616D) were added to 200 μL supernatant, respectively. Beads were then magnetically separated after overnight shaking at 4°C, washed with PBS three times, and were labeled with FITC-anti-CD81 or PE-anti-CD63 for 20 minutes.

In some experiments, the EV pellet after UC was resuspended in 500 μL PBS and incubated with anti-CD63 coated beads overnight. After washing, primary antibodies against EGF family members were applied in 50 μL PBS + 1% BSA for 2 hours at room temperature (RT), and the Alexa 488-labeled secondary antibodies were used for 1 hour. Ten thousand beads were measured with a FACSCalibur instrument (BD Biosciences).

2.11 | Mouse EV detection by anti-CD81-coated beads

Ten microliters of anti-CD81 antibody were bound to 2 mg magnetic beads by the Dynabeads Antibody Coupling Kit (Invitrogen-Thermo Fisher Scientific) according to the manufacturer's instructions. One microliter of the antibody-coated beads was applied to 200 μL supernatant. Beads with EVs were detected by PE-anti-CD81 antibody, and the percentage of positive beads was measured by flow cytometry.

2.12 | Immunostaining

Paraffin-embedded tissue blocks from the intestines of mice were cut. The 4 μm sections were deparaffinized; they were treated with high pH target retrieval solution (Tris-EDTA buffer with 10 mM Tris base, 1 mM EDTA solution, 0.05% Tween 20, pH 9.0) in a microwave oven at 700 W for 5 minutes and at 400 W for 10 minutes. For immunostaining, the sections were blocked in 0.1 M TrisHCl, 0.15 M NaCl, 2% FBS for 30 minutes, and the primary antibody was used overnight at 4°C. The sections were then washed with TNT buffer (0.1 M TRIS pH = 7.4, 0.15 M sodium chloride, 0.05% Tween20), incubated with secondary antibodies for 1 hour at RT and mounted with ProLong Diamond antifade mountant containing DAPI (Thermo Fisher Scientific).

For immunostaining of cells, they were fixed in 4% PFA for 20 minutes, blocking and permeabilization were carried out in blocking buffer (PBS with 0.1% BSA, 5% FBS and 0.1% Triton X-100). After washing with blocking buffer, cells were incubated with primary antibodies at 4°C overnight and then in secondary antibodies for 2 hours at RT in blocking buffer. Samples were covered with ProLong Diamond antifade mountant containing DAPI (Thermo Fisher Scientific), and they were imaged with a Nicon Eclipse 80i fluorescent microscope.

2.13 | Whole-mount staining

Organoids were cultured in 4-well or 8-well chamber slides (BD Biosciences), fixed in 4% PFA for 30 minutes, washed with PBS and blocked and permeabilized in whole-mount blocking buffer (WMBB: 5% FBS, 0.2% BSA, 0.3% Triton X-100 in PBS) for 30 minutes. Primary antibodies were used at 4°C overnight in WMBB. After washing in PBS + 0.3% Triton X-100 + 4% NaCl and overnight incubation with labeled secondary antibodies, the organoids were mounted with ProLong Diamond antifade mountant containing DAPI (Thermo Fisher Scientific) and imaged with a Zeiss LSM800 confocal microscope. Images were processed by the ImageJ software.

2.14 | Statistical analysis

Student's paired or unpaired *t*-test, analysis of variance, and Tukey post hoc test or Kruskal-Wallis with Dunn post hoc test were used with $*P < .05$, $**P < .01$, and $***P < .005$ significance levels. Microsoft Excel and SPSS version 25 software were used for statistical evaluation. Mean and SD values are shown with n = 3-5 biological replicates, unless otherwise indicated.

3 | RESULTS

3.1 | Intestinal fibroblasts secrete EVs

To study the EV-mediated signal transmission in the ISC niche, we used commercially available normal HCFs and isolated intestinal fibroblasts from C57Bl/6J mice (murine small intestinal fibroblast—MIF) as well. HCF cultures were uniformly positive for αSma (Figure S1a,b), thus, confirming the purity of the cultures. Previous studies have shown that beads coated with antibodies specific for EV markers, such as CD63 or CD81, can capture EVs from cell and organoid culture supernatant and they can then be detected by flow cytometry.[15,16] We detected EVs from HCFs with anti-CD63 or anti-CD81-coated beads (Figure S1c,d) and, importantly, beads covered with streptavidin were unable to bind EVs, thus, confirming the specificity of the method (Figure S1d). In addition, EVs bound to anti-CD63-coated beads were negative for

Annexin V, a marker of some specific larger EV populations (Figure S1d). Transmission electron microscopy proved the presence of EVs in the ultracentrifuged pellet of HCF-derived supernatant (Figure S1e); furthermore, tunable resistive pulse sensing and nanoparticle tracking analysis that are standard methods for EV characterization, showed the shift of EV size toward the smaller range in EV preparates (Figure S1f,g). Similarly, MIF cultures were positive for αSma (Figure S1h), and CD81+ EVs were detected in their culture supernatants by antibody-coated beads (Figure S1i). Collectively, these data show that both human and mouse intestinal fibroblasts secrete EVs into the culture medium.

3.2 | Intestinal fibroblast-derived EVs do not modify ISC activity in the presence of exogenously added ISC niche factors

ISCs reside at the crypt bottoms; they are responsible for maintaining the crypt structure and for producing all other intestinal epithelial cell types, leading to the budding of the organoids. Thus, counting the living, budding, or dead organoids provides a robust and easy method to detect ISC activity. The exogenously added EGF, the Bmp inhibitor noggin, and the Wnt-agonist R-Spondin1 are critical for maintaining the ISC population in small intestinal (SI) organoids.[4] Importantly, when the medium from HCFs was ultracentrifuged, the pellet fraction, but not the supernatant, contained EVs (Figure S2a). Interestingly, the concentrated HCF or MIF-derived EVs, isolated by UC, did not influence the number of surviving or budding SI organoids (Figure S2b-c). Thus, neither colon nor small intestinal fibroblast-derived EVs carry molecules that could have an additional or inhibitory effect in the formation of the ISC niche when all the essential niche factors are present.

3.3 | Fibroblast-derived EVs do not modify the effect of IFNγ or TNFα acting in the ISC niche

To test whether fibroblast-derived EVs have a combinatorial effect with other factors acting in the ISC niche, we selected TNFα and IFNγ, since they have a well-known effect on ISCs and/or the intestinal crypt region and both play a central role in the intestinal immune responses.[17,18] As expected, IFNγ led to the death of SI organoids[18] and TNFα resulted in the appearance of cyst-like organoids without modifying the proportion of active caspase-3+ apoptotic cells (Figure S2d-f).[17] Interestingly, however, the addition of fibroblast-derived EVs did not have any rescue effect on these measured parameters either with IFNγ or in the presence of TNFα (Figure S2d-f).

3.4 | Fibroblast-derived EVs carry EGF activity in the ISC niche

Wnt factors are highly hydrophobic, and a recent work reported that Wnt activity is enhanced when they are added in liposomes.[19] To study whether some of the niche factors travel on EVs, first we focused on Wnt proteins in the ISC niche. In contrast to SI organoids where Paneth cells produce Wnt proteins, colon organoids critically depend on external Wnt factors in cultures due to the lack of this cell type.[3] HCF-derived EVs showed a marked rescue effect in colon organoid survival when Wnt3a lacked from the culture medium (Figure 1A,B), demonstrating that EVs critically contribute to the normal Wnt activity in the ISC niche.

To test whether some of the other critical ISC niche factors are transmitted by fibroblast-derived EVs, we removed R-Spondin1, noggin or EGF from culture medium. As expected, the lack of one of these factors led to a markedly reduced organoid survival at day 4, showing the disappearance of ISC function (Figure 2A-C). Interestingly, whereas fibroblast EVs did not rescue the reduced survival of organoids when R-Spondin1 or noggin lacked (Figure 2A), we observed an extensive rescue effect for EGF not only in SI, but in colon organoids as well when applying HCF EVs (Figure 2B-D). Importantly, we confirmed this effect in SI organoids with MIF-derived EVs (Figure 2E), suggesting that both colonic and small intestinal fibroblasts are able to deliver EGF activity. Similarly, fibroblast-derived EVs restored the proportion of the Ki67+ proliferating and active caspase-3+ apoptotic cells when EGF lacked from the medium (Figure 2F-H).

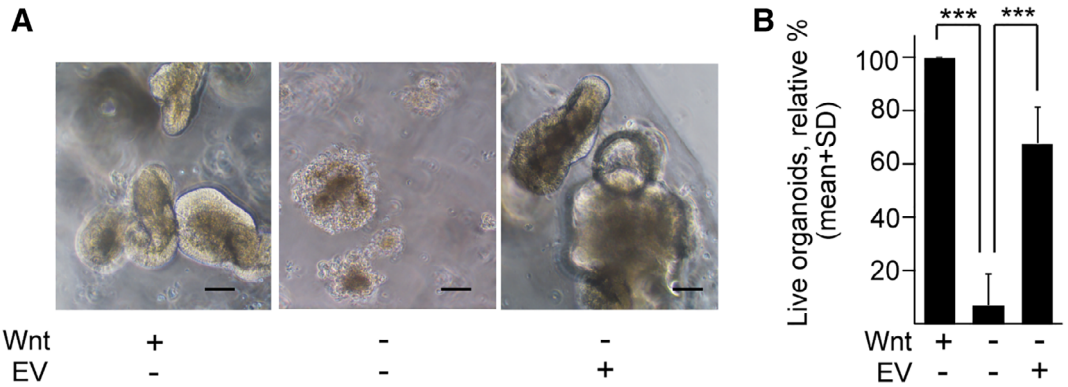

FIGURE 1 Fibroblast-derived extracellular vesicles (EVs) restore colonic organoid survival when external Wnt proteins are absent. A, Representative images in the presence or absence of Wnt3a (100 ng/mL) and human colon fibroblast-derived EVs (scale bars: 20 μm). B, Quantification of the living colonic organoids. Treatments were started at the time of organoid splitting and organoids were counted on day 4 (n = 3, mean + SD, analysis of variance and Tukey post hoc test, ***$P < .005$)

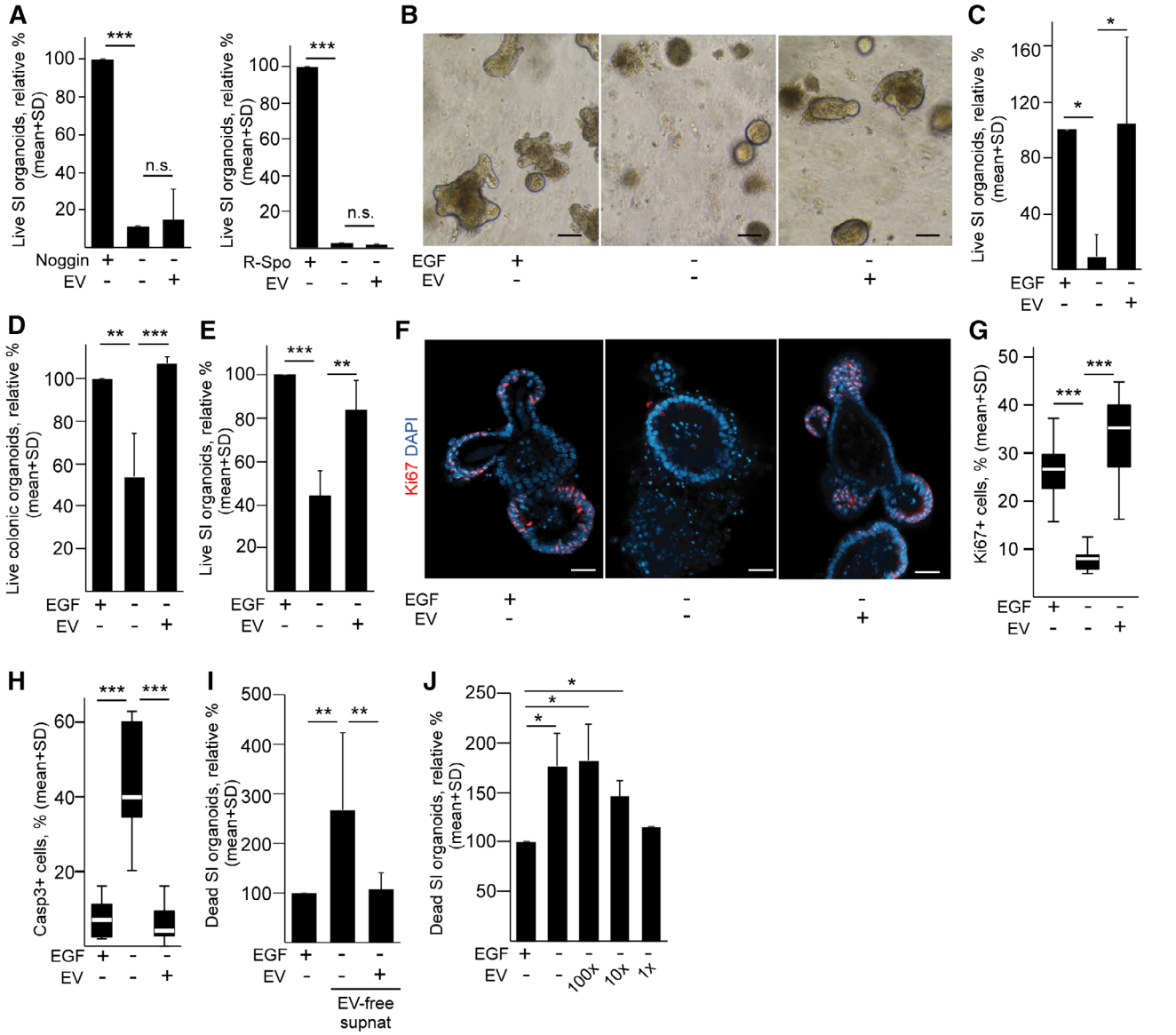

FIGURE 2 Fibroblast-derived extracellular vesicles (EVs) transmit epidermal growth factor (EGF) activity in the intestinal stem cell niche. A, Surviving small intestinal (SI) organoids 4 days after removing noggin or R-Spondin1 and/or adding human colon fibroblast (HCF)-derived EVs (n = 3). B and C, Representative images (B) from SI organoids when EGF was removed or HCF-derived EVs were added and the quantification at day 4 (C) (n = 5). D, The proportion of living colonic organoids with the indicated treatments. EVs were pelleted from HCF supernatants (n = 3). E, Quantification of the living SI organoids at day 4 when EGF was absent or mouse small intestinal fibroblast (MIF)-derived EVs were added (n = 3). F and G, Representative images (F) and the quantification of Ki67^{+} proliferating cells (G) from SI organoids in the absence of EGF or the presence of HCF-derived EVs at day 4 (n = 10-12 from three experiments). H, The percentage of active caspase-3^{+} apoptotic cells in SI organoids with the indicated treatments at day 3 (n = 10-12 from three experiments). I, The relative percentage of dead SI organoids when HCF-derived supernatant was applied after ultracentrifugation (UC). Note that UC removes EVs from the supernatant. EGF or the UC-pelleted EVs with the EV-depleted UC supernatant were added to some organoids (n = 3). J, Dead organoid rate when HCF-derived EVs were applied at different dilutions (1×, 10×, 100×) in the absence of EGF (n = 3). Kruskal-Wallis test and Dunn post hoc test (G, H) or analysis of variance and Tukey post hoc test (A, C, D, E, I, J) were used. Scale bars: 50 μm, $^{*}P < .05$, $^{**}P < .01$, $^{***}P < .005$, n.s., not significant

Furthermore, a significant increase in the percentage of dead organoids was observed when HCF-derived EVs were removed from the supernatant, and this was restored in the presence of EVs (Figure 2I), suggesting that EGF activity is largely connected to EVs in fibroblast supernatants. In addition, HCF-derived EVs showed a dose-dependent effect on the death of organoids when EGF lacked from the culture medium (Figure 2J). Importantly, HCF-derived EVs prevented organoid death when EGF lacked in human colon organoid cultures, thus, confirming that EGF activity can be transmitted via EVs in the human ISC niche as well (Figure S3).

To further prove that EGF activity may be transmitted by EVs in the ISC niche, we carried out immunostaining for phospho-EGF receptor and observed the rescue effect of EVs in the absence of exogenously added EGF (Figure S4a). As expected, crypt cells, but not the villi, were positive

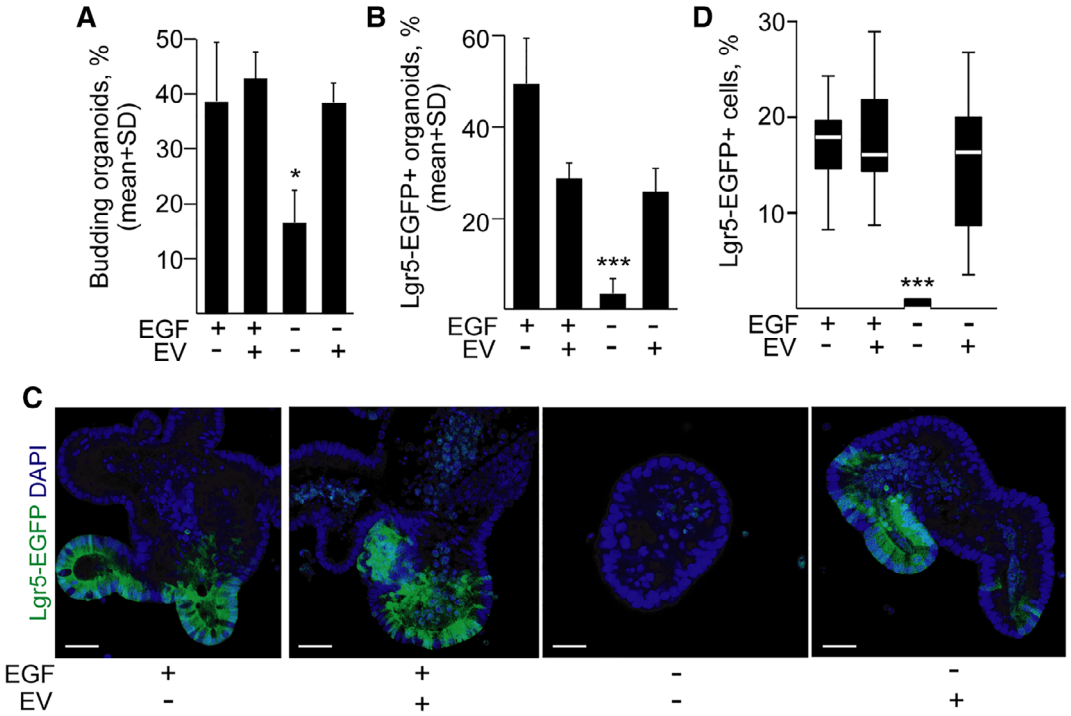

FIGURE 3 Fibroblast-derived extracellular vesicles (EVs) restore the Lgr5-EGFP$^+$ intestinal stem cell population in the absence of epidermal growth factor (EGF). A, The percentage of Lgr5-EGFP organoids with more than two budding structures at day 4 after the indicated treatments. EVs were isolated from human colon fibroblasts (n = 4). B, The proportion of organoids with EGFP$^+$ cells (n = 4). CHIR99021 was applied 3 days before treatments. C, Representative confocal microscopic images, taken 4 days after removing EGF and/or adding EVs (scale bars: 50 μm). D, The percentage of EGFP$^+$ cells in the organoids (n = 10-11 from three experiments). Analysis of variance and Tukey post hoc tests (A, B) or Kruskal-Wallis and Dunn post hoc tests (D) were used. * and *** indicate $P < .05$ and $P < .005$, respectively, compared with all other groups. Mean + SD (A, B) or minimum, Q1, median, Q3, and maximum (D) are shown

for phospho-EGFR immunostaining in mouse intestinal tissue sections (Figure S4b), thus, confirming the specificity of our staining protocol. In addition, we used the EGF receptor inhibitor gefitinib as well. Similar to the exogenously added soluble EGF, the rescue effect of EVs was blocked in the presence of the inhibitor (Figure S4c).

We next isolated SI organoids from *Lgr5-EGFP-IRES-Cre^{ERT2}* mice, expressing the green fluorescent protein EGFP in ISCs.[1] To expand the EGFP$^+$ green ISC population in the SI organoids, we applied the GSK3 inhibitor CHIR99021 that activates the Wnt pathway.[20] We detected a massively reduced organoid budding and a decrease in the proportion of EGFP$^+$ organoids when EGF was removed from culture medium and, importantly, this effect was rescued by fibroblast-derived EVs (Figure 3A,B). Interestingly, EGFP+ cells completely disappeared when EGF lacked; however, we could still detect green cells in SI organoids when the culture medium was supplemented with HCF-derived EVs (Figure 3C-D), further proving that EGF activity is preferentially transmitted via EVs in the ISC niche.

3.5 | Fibroblast-derived EVs carry amphiregulin in the ISC niche

The Vesiclepedia database (http://microvesicles.org/) contains molecular data from isolated EVs. To determine which EGF family members may be transmitted by EVs, we selected proteomics datasets derived from cell cultures. As expected, known EV markers (CD9, CD63, CD81) were represented in a high percentage of the data sets (Figure S5a). Interestingly, we observed a similarly high representation of Wnt proteins and the lack of R-Spondins in these lists (Figure S5a). When focusing on EGF family members, epiregulin (EREG), TGFα, and amphiregulin (AREG) were present in some cell line-derived EVs. However, all these hits derived only from cancer cells (Figure S4a). Thus, analysis of Vesiclepedia data suggested that EGF family members, such as epiregulin, TGFα, and amphiregulin may be transmitted by EVs; however, it did not give any indication for their presence on EVs of non-cancerous cell origin.

Reverse transcription quantitative PCR showed that both HCFs and MIFs expressed a wide array of EGF ligands, such as EGF, betacellulin, amphiregulin, epiregulin, and HBEGF, although the relative mRNA level of the family members varied between mouse and human cells (Figure 4A,B). In contrast, the RNA level of these molecules was very low or undetectable in SI organoids (Figure 4B). EVs isolated by anti-CD63 antibody-coated beads from fibroblast cultures were positive for amphiregulin (Figure 4C,D), and we detected amphiregulin in the HCF-derived EV pellet by Western blotting as well (Figure 4E), showing that at least this member of the EGF ligand family is transported by fibroblast-derived EVs in the ISC niche. Importantly, the bead-based experiment also confirms that EGF activity of

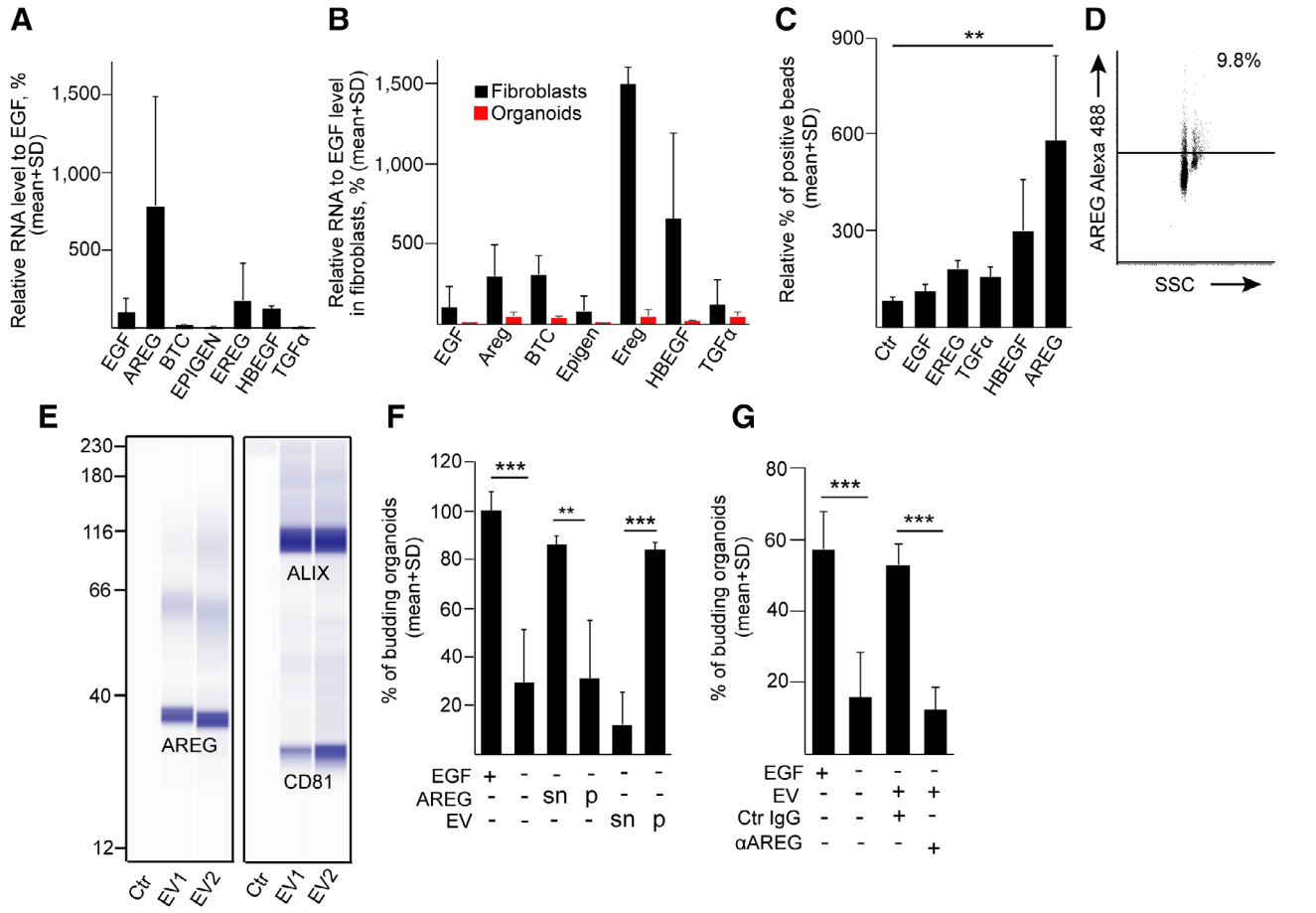

FIGURE 4 Epidermal growth factor (EGF) family members are present on extracellular vesicles (EVs). A, The relative RNA levels of EGF family members in human colon fibroblasts (HCFs) (n = 3, RT-qPCR). Expression levels normalized to HPRT1 housekeeping were compared with the relative level of EGF. B, Expression levels of EGF family members in murine small intestinal fibroblast (MIFs) and small intestinal organoids. The Hprt-normalized Egf RNA in MIFs was taken as 100% (n = 3, RT-qPCR). C and D, The relative percentage of positive anti-CD63-coated beads after incubating with HCF-derived EVs and detected with antibodies against the indicated EGF family members (C) and selected flow cytometry dot plot when using anti-ampiregulin (AREG) antibody (D). EVs were pelleted by ultracentrifugation and dissolved in phosphate-buffered saline (n = 3, ctr: Sample with control primary antibody). E, Simple Western WES analysis of two HCF-derived ultracentrifuged supernatants (EV1, EV2) for AREG (34 kDa) and the EV markers CD81 (29 kDa) and ALIX (108 kDa). The control sample was prepared from medium. F, The percentage of budding organoids when medium containing amphiregulin (AREG, 50 ng/mL) or HCF-derived samples (EV) were ultracentrifuged, and the supernatants (sn) and the pellets (*P*) were applied (n = 3). Note that AREG was not ultracentrifuged from the medium. G, The proportion of budding organoids when HCF-derived EVs were pre-incubated with control or neutralizing anti-amphiregulin antibody before applying them to organoids (n = 5). Analysis of variance and Tukey post hoc tests were used (C, F, G). Mean + SD are shown, $^{**}P < .01$, $^{***}P < .005$

the UC pellet is not just an unspecific co-purification event during EV isolation. As another experiment, we added amphiregulin to the medium, and the supernatants and pellets after UC were applied in SI organoid cultures. Interestingly, this supernatant, but not the pellet, had a rescue effect on organoid death, showing that exogenously added amphiregulin does not co-purify with medium components (Figure 4F).

The used antibodies for EGF family members recognize the extracellular domains of the growth factors (see Materials and Methods in Supporting Information Appendix), suggesting that EV-bound amphiregulin is able to bind to its receptor. Indeed, when neutralizing amphiregulin in fibroblast-derived EVs before applying them to organoids in the absence of EGF, we observed a marked reduction in the proportion of budding organoids, showing the reduced stem cell activity (Figure 4G). Collectively, fibroblast-derived EVs carry active amphiregulin as EGF activity in the ISC niche.

3.6 | Fibroblast-derived EVs have no role in maintaining the stem cell niche when EGF is dispensible

Apc mutation represents one of the first genetic events in colorectal tumorigenesis, leading to adenoma formation. Mouse intestinal adenoma organoids are independent of ISC factors, including EGF family members.[13,21] To study the role of fibroblast-derived EVs in an EGF-independent model, we used *Apc*-mutant SI organoids that had been created previously by the CRISPR-Cas9 technology and had been

selected in the absence of the niche factors, including R-Spondin1.[15] Interestingly, whereas HCF-derived supernatant had a dramatic effect on the colony forming efficiency of Apc-mutant cells (Figure S5b), this increase was not attributed to either EGF or EVs (Figure S5b-c), as proved by adding supernatant or the pellet after UC. Thus, similarly to EGF, fibroblast-derived EVs have a critical role in maintaining the normal ISC stem cell niche, but they are dispensible for mouse intestinal adenoma cells.

4 | DISCUSSION

We show here that both colonic and small intestinal fibroblast-derived EVs play a critical role in the transmission of EGF activity in the normal ISC niche. Importantly, our data prove that at least one EGF member, amphiregulin, can travel via EVs from fibroblasts to ISCs. Furthermore, fibroblast-derived EVs can rescue the lack of Wnt proteins as well. However, when all the essential niche factors were present, EVs did not modify the survival of intestinal crypts.

The highly hydrophobic Wnt proteins are critical factors in the ISC niche. Farin et al have found that ISC membranes constitute a reservoir for Wnt proteins and Wnt3 mainly travels away from its source in a cell-bound manner through cell division, but how it is transferred between producing and receiving cells has not been identified.[10] Interestingly, a recent study reported that within the epithelium, dying cells release Wnt-containing apoptotic bodies that regulate stem cell proliferation.[22] Others have proved that Wnt proteins may travel via EXs, the endosome-derived subpopulation of EVs in the intercellular space.[23] The relevance of this finding has been proved in many models, such as pulmonary fibrosis or heart diseases.[24-26] Wnts may bind to lipoproteins that stabilize them as well.[19,27] Interestingly, macrophage-derived EVs carry Wnt proteins to ISCs in intestinal repair,[11] and we provide evidence that fibroblast-derived EVs transfer Wnt activity in the ISC niche in WT organoids as well. Importantly, we found no rescue effect with EVs when R-Spondin1 lacked from the culture medium. R-Spondin1 represents a major amplification step in the Wnt signaling pathway by binding to the ISC marker Lgr5.[28] Fibroblast-derived EVs contribute to the regulation of Wnt activity in the normal ISC niche via transmitting some but not all ligands of this pathway. Thus, EVs are predicted not to be able to fully and completely activate the Wnt pathway.

EGF receptor ligand family members are synthesized as membrane-bound molecules and can then be released after cleavage by proteases. Interestingly, members of the EGF family, including amphiregulin, may act in a paracrine, autocrine, and juxtacrine manner.[29,30] Our results agree with a previous report, showing that some EGF family members, such as amphiregulin, are transported by EVs and that amphiregulin is present as a full-length, membrane-bound form on EVs.[31] Importantly, this study also proved that EV-bound amphiregulin and HB-EGF are approximately fivefold more efficient compared with recombinant proteins.[31] The presence of the full-length amphiregulin on different EV subpopulations has been confirmed by other reports as well.[32-34] However, all these studies used cancer cell lines and some of them only analyzed the molecular cargo of EVs. To our knowledge, this is the first report to prove the role of fibroblast-derived EVs in the transmission of EGF activity, such as amphiregulin, among non-cancer cells in an organoid system, modeling the ISC niche. Since neutralizing EV-bound amphiregulin blocked the effects of fibroblast-derived EVs, this indicates that EGF family members, such as amphiregulin, are present on the surface of EVs in the proper orientation, and we also provide evidence that EVs activate EGF receptors. Furthermore, our data suggest that although recombinant EGF is effective in intestinal organoid cultures, fibroblast-derived EGF activity is connected to EVs in the ISC niche, providing a concentrated way of transmission. Interestingly, the maintenance of the stem cell population requires high activity of ISC niche factors, such as Wnt[28]; thus, transmission via EVs is a tool to provide the necessary concentration of these factors.

5 | CONCLUSION

Collectively, our data show that colonic and small intestinal fibroblast-derived EVs carry EGF family members, such as amphiregulin that act as niche factors for ISCs; thus, EVs contribute to the maintenance of the ISC phenotype. Since providing niche factors is important not only under homeostasis but after intestinal injuries as well, EVs may contribute as a novel tool to develop better regenerating strategies by transporting niche factors in diseases where the ISC niche is disturbed.

ACKNOWLEDGMENTS

The authors thank all members of the Extracellular Vesicle Research Group of Semmelweis University for their technical help and to Zoltán Varga (Institute of Materials and Environmental Chemistry, Hungarian Academy of Sciences) for providing resources for TEM imaging. This work was financed by the Collaborative Research Programme (CRP/HUN16-04_EC, International Centre for Genetic Engineering and Biotechnology, Italy), by OTKA-NN 118018, OTKA 111958, 120237 and the National Competitiveness and Excellence program NVKP_16-0007 (National Research, Development and Innovation Office, Hungary), by VEKOP-2.3.2-16-2017-000002, VEKOP-2.3.3-15-2017-00016 and by the National Excellence Program in Higher Education (Ministry of Human Capacities, Hungary).

AUTHOR CONTRIBUTIONS

Á.O.: conception and design, collection and/or assembly of data, data analysis and interpretation, manuscript writing; Z.S.: collection and/or assembly of data; G.O.S.: collection and/or assembly of data; A.K.: collection and/or assembly of data; A.Á.S.: collection and/or assembly of data; K.P.: collection of data; A.B.: provision of study material or patients; K.D.: provision of study material or patients; T.T.: provision of study material or patients; E.I.B.: data analysis and interpretation; A.Z.: data analysis and interpretation, collection and/or assembly of data; Z.W.: conception and design, financial support, data analysis and interpretation, manuscript writing, final approval of manuscript.

CONFLICT OF INTEREST

The authors declare no potential conflict of interest.

DATA AVAILABILITY STATEMENT

The data supporting results in this study are available from the corresponding author upon reasonable request.

ORCID

Zoltán Wiener https://orcid.org/0000-0001-7056-4926

REFERENCES

1. Barker N, van Es JH, Kuipers J, et al. Identification of stem cells in small intestine and colon by marker gene Lgr5. *Nature*. 2007;449:1003-1007.
2. de Lau W, Barker N, Low TY, et al. Lgr5 homologues associate with Wnt receptors and mediate R-spondin signalling. *Nature*. 2011;476:293-297.
3. Sato T, Stange DE, Ferrante M, et al. Long-term expansion of epithelial organoids from human colon, adenoma, adenocarcinoma, and Barrett's epithelium. *Gastroenterology*. 2011;141:1762-1772.
4. Sato T, Vries RG, Snippert HJ, et al. Single Lgr5 stem cells build crypt-villus structures in vitro without a mesenchymal niche. *Nature*. 2009;459:262-265.
5. Gyorgy B, Szabo TG, Pasztoi M, et al. Membrane vesicles, current state-of-the-art: emerging role of extracellular vesicles. *Cell Mol Life Sci*. 2011;68:2667-2688.
6. Kowal J, Arras G, Colombo M, et al. Proteomic comparison defines novel markers to characterize heterogeneous populations of extracellular vesicle subtypes. *Proc Natl Acad Sci U S A*. 2016;113:E968-E977.
7. Buzas EI, Gyorgy B, Nagy G, et al. Emerging role of extracellular vesicles in inflammatory diseases. *Nat Rev Rheumatol*. 2014;10:356-364.
8. Ragni E, Banfi F, Barilani M, et al. Extracellular vesicle-shuttled mRNA in mesenchymal stem cell communication. *Stem Cells*. 2017;35:1093-1105.
9. Liu S, Mahairaki V, Bai H, et al. Highly purified human extracellular vesicles produced by stem cells alleviate aging cellular phenotypes of senescent human cells. *Stem Cells*. 2019;37:779-790.
10. Farin HF, Jordens I, Mosa MH, et al. Visualization of a short-range Wnt gradient in the intestinal stem-cell niche. *Nature*. 2016;530:340-343.
11. Saha S, Aranda E, Hayakawa Y, et al. Macrophage-derived extracellular vesicle-packaged WNTs rescue intestinal stem cells and enhance survival after radiation injury. *Nat Commun*. 2016;7:13096.
12. Leoni G, Neumann PA, Kamaly N, et al. Annexin A1-containing extracellular vesicles and polymeric nanoparticles promote epithelial wound repair. *J Clin Invest*. 2015;125:1215-1227.
13. Sato T, van Es JH, Snippert HJ, et al. Paneth cells constitute the niche for Lgr5 stem cells in intestinal crypts. *Nature*. 2011;469:415-418.
14. Schwank G, Koo BK, Sasselli V, et al. Functional repair of CFTR by CRISPR/Cas9 in intestinal stem cell organoids of cystic fibrosis patients. *Cell Stem Cell*. 2013;13:653-658.
15. Szvicsek Z, Oszvald A, Szabo L, et al. Extracellular vesicle release from intestinal organoids is modulated by Apc mutation and other colorectal cancer progression factors. *Cell Mol Life Sci*. 2019;76:2463-2476.
16. Ostrowski M, Carmo NB, Krumeich S et al. Rab27a and Rab27b control different steps of the exosome secretion pathway. *Nat Cell Biol* 2010;12:19–30; sup pp 1–13.
17. Pribluda A, Elyada E, Wiener Z, et al. A senescence-inflammatory switch from cancer-inhibitory to cancer-promoting mechanism. *Cancer Cell*. 2013;24:242-256.
18. Farin HF, Karthaus WR, Kujala P, et al. Paneth cell extrusion and release of antimicrobial products is directly controlled by immune cell-derived IFN-gamma. *J Exp Med*. 2014;211:1393-1405.
19. Tuysuz N, van Bloois L, van den Brink S, et al. Lipid-mediated Wnt protein stabilization enables serum-free culture of human organ stem cells. *Nat Commun*. 2017;8:14578.
20. Yin X, Farin HF, van Es JH, Clevers H, Langer R, Karp JM. Niche-independent high-purity cultures of Lgr5+ intestinal stem cells and their progeny. *Nat Methods*. 2014;11:106-112.
21. Wiener Z, Hogstrom J, Hyvonen V, et al. Prox1 promotes expansion of the colorectal cancer stem cell population to fuel tumor growth and ischemia resistance. *Cell Rep*. 2014;8:1943-1956.
22. Brock CK, Wallin ST, Ruiz OE, et al. Stem cell proliferation is induced by apoptotic bodies from dying cells during epithelial tissue maintenance. *Nat Commun*. 2019;10:1044.
23. Gross JC, Chaudhary V, Bartscherer K, Boutros M. Active Wnt proteins are secreted on exosomes. *Nat Cell Biol*. 2012;14:1036-1045.
24. Martin-Medina A, Lehmann M, Burgy O, et al. increased extracellular vesicles mediate WNT-5a signaling in idiopathic pulmonary fibrosis. *Am J Respir Crit Care Med*. 2018;198:1527-1538.
25. Gross JC, Zelarayan LC. The mingle-mangle of Wnt signaling and extracellular vesicles: functional implications for heart research. *Front Cardiovasc Med*. 2018;5:10.
26. Dzialo E, Rudnik M, Koning RI, et al. WNT3a and WNT5a Transported by Exosomes Activate WNT Signaling Pathways in Human Cardiac Fibroblasts. *Int J Mol Sci*. 2019;20:E1436.
27. Kaiser K, Gyllborg D, Prochazka J, et al. WNT5A is transported via lipoprotein particles in the cerebrospinal fluid to regulate hindbrain morphogenesis. *Nat Commun*. 2019;10:1498.
28. de Lau W, Peng WC, Gros P, Clevers H. The R-spondin/Lgr5/Rnf43 module: regulator of Wnt signal strength. *Genes Dev*. 2014;28:305-316.
29. Singh AB, Harris RC. Autocrine, paracrine and juxtacrine signaling by EGFR ligands. *Cell Signal*. 2005;17:1183-1193.
30. Berasain C, Avila MA. Amphiregulin. *Semin Cell Dev Biol*. 2014;28:31-41.
31. Higginbotham JN, Demory Beckler M, Gephart JD, et al. Amphiregulin exosomes increase cancer cell invasion. *Curr Biol*. 2011;21:779-786.
32. Raimondo S, Saieva L, Vicario E, et al. Multiple myeloma-derived exosomes are enriched of amphiregulin (AREG) and activate the epidermal growth factor pathway in the bone microenvironment leading to osteoclastogenesis. *J Hematol Oncol*. 2019;12:2.
33. Taverna S, Pucci M, Giallombardo M, et al. Amphiregulin contained in NSCLC-exosomes induces osteoclast differentiation through the activation of EGFR pathway. *Sci Rep*. 2017;7:3170.
34. Zhang Q, Higginbotham JN, Jeppesen DK, et al. Transfer of functional cargo in exomeres. *Cell Rep*. 2019;27:940-954.e6.

SUPPORTING INFORMATION

Additional supporting information may be found online in the Supporting Information section at the end of this article.

How to cite this article: Oszvald Á, Szvicsek Z, Sándor GO, et al. Extracellular vesicles transmit epithelial growth factor activity in the intestinal stem cell niche. *Stem Cells*. 2019;1–10. https://doi.org/10.1002/stem.3113